Sensitized Lanthanide-Ion Luminescence with Aryl-Substituted *N*-(2-Nitrophenyl)acetamide-Derived Chromophores

by **Michael Andrews**[a]), **Benjamin D. Ward**[a]), **Rebecca H. Laye**[b]), **Benson M. Kariuki**[a]), and **Simon J. A. Pope***[a])

[a]) School of Chemistry, Main Building, Cardiff University, Park Place, Cardiff, UK CF10 3AT (phone: +44-2920879316; fax: +44-2920874030; e-mail: popesj@cardiff.ac.uk)

[b]) Department of Chemistry, University of Sheffield, Sheffield, UK

Dedicated to Prof. *Jean-Claude Bünzli* on the occasion of his 65th birthday

The syntheses of the two tetraazamacrocyclic ligands **L1** and **L2** bearing a [(methoxy-2-nitrophenyl)amino]carbonyl chromophore, *i.e.*, an *N*-(methoxy-2-nitrophenyl)acetamide moiety, together with their corresponding lanthanide-ion complexes are described. A combined spectroscopic (UV/VIS, ^{1}H-NMR), structural (X-ray), and theoretical (DFT) investigation revealed that the absorption properties of the chromophores were dictated by the extent of electronic delocalisation, which in turn was determined by the position of the MeO substituent at the aromatic ring. X-Ray crystallographic studies showed that when attached to the macrocycle, both isomeric forms of the *N*-(methoxy-2-nitrophenyl)acetamide unit can participate in coordination, *via* the C=O, to an encapsulated potassium cation. Luminescence measurements confirmed that such a binding mode also exists in solution for the corresponding lanthanide complexes (*q ca.* ≤ 1), with the *para*-MeO derivative allowing longer wavelength sensitization (λ_{ex} 330 nm).

Introduction. – The rich and diverse synthetic organic chemistry associated with functionalised aromatics can be exploited in the design of luminescent lanthanide complexes [1]. Since lanthanide luminescence arises from forbidden *f*–*f* transitions, the use of a sensitising chromophore is required to facilitate and optimise the emission properties. From a purely energetic perspective, the choice of chromophore for visibly emitting lanthanides such as Eu^{III} and Tb^{III} is far more limited than for near-IR emitters such as Nd^{III}, Er^{III}, and Yb^{III}. However, the exploitation of lanthanide complexes in the field of biological imaging, specifically confocal fluorescence microscopy [2], has driven the rapid development of synthetic strategies aimed toward optimising biocompatible optical and photophysical properties. Several research groups have usefully exploited a wide range of organic aromatic chromophores which allow reasonable long-wavelength sensitization of various emissive lanthanide ions. Such species can be based upon functionalised aromatics such as xanthone [3], acridone [4], pyrene [5], or quinoxaline [6] amongst other notable examples [7]. Chromophores with red-shifted absorption properties can also encompass charge-transfer species based upon transition metal complexes such as Cr^{III} [8], Ru^{II} [9], Re^{I} [10], Os^{II} [11], Ir^{III} [12], and Pt^{II} [13]. More recently, *Bünzli* and co-workers have used 'push-pull' aromatic diketonato ligands incorporating electron-donating and electron-withdrawing units, allowing the possibility of intra-ligand charge transfer (ILCT) excited states to be

usefully exploited as a means of sensitisation [14]. In this context, simple nitrophenol-derived aromatics represent a potentially useful class of comparable chromophores [15]. Indeed poly-fluorinated nitrophenoxide ligands have been exploited in sensitized near-IR emitting species [16]. Substituted acetophenone chromophores with varying elements of charge-transfer character have also been employed to sensitise Eu^{III} [17]. In this article, we describe the synthetic exploitation of two [(2-nitrophenyl)amino]-carbonyl-derived chromophores *i.e.*, *N*-(2-nitrophenyl)acetamide-derived chromophores, within an azamacrocyclic framework yielding H_2O-soluble lanthanide complexes, together with their resultant sensitized VIS and near-IR emission.

Results and Discussion. – *Synthesis and Characterisation of the Ligand Precursors and Ligands.* Prior to covalent attachment to the azamacrocycle, the chromophores were derivatised as 2-chloroacetamides. Although it was possible to isolate the nitrophenol-derived 2-chloroacetamide **1b** (*Scheme*) by reaction of the 2-amino-3-nitrophenol with 2-chloroacetyl chloride (the X-ray crystal structure of **1b** (*Fig. 1*) is discussed below), further reaction with base (either for the attempted methylation or coupling with the macrocycle), not unexpectedly, yielded the intramolecularly cyclised acetamide, identified by ESI-MS (*m*/*z* 194 ($[M+H]^+$)) and ^{1}H-NMR (unique resonances for the CH_2 and NH moieties at δ(H) 4.64 and 9.99, resp.) rather than the desired product. Consequently, for both isomers, the phenol groups were selectively methylated with MeI in acetone in the presence of K_2CO_3 (*Scheme*). Subsequent reaction of the methylated intermediates with 2-chloroacetyl chloride yielded the 2-chloro-*N*-(2-methoxy-6-nitrophenyl)acetamide (**1a**) as a beige solid and the 2-chloro-

Scheme. *Synthetic Pathway to the 2-Chloroacetamides*

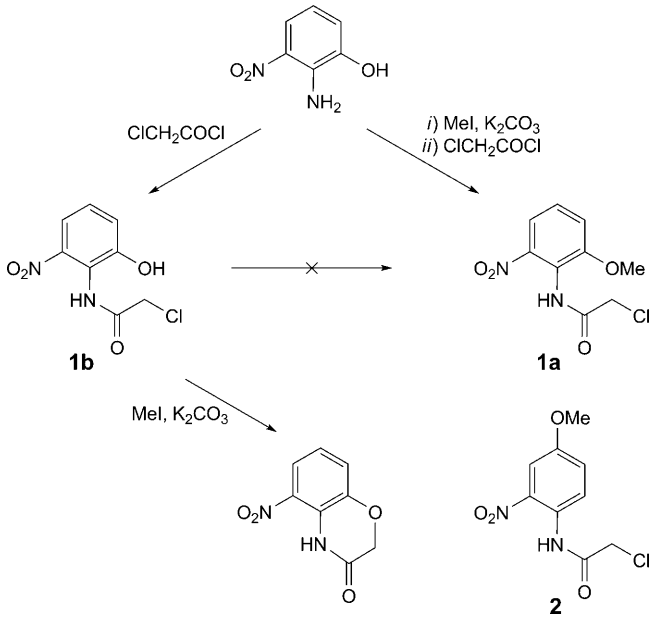

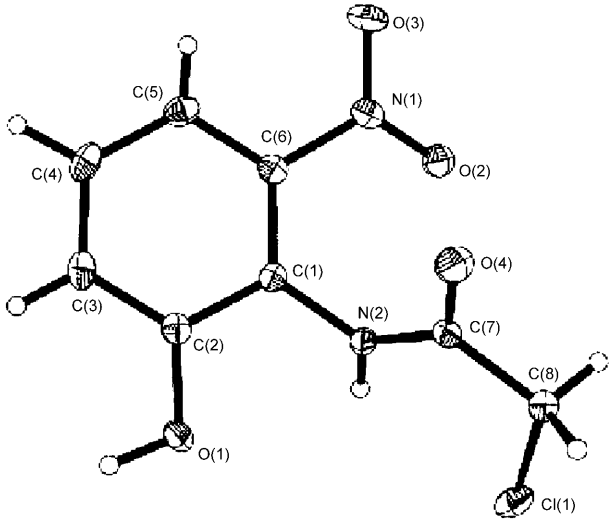

Fig. 1. *X-Ray-structure representation of* **1b**. Solvent molecules of crystallisation are omitted for clarity. Probability ellipsoids set at 50%.

N-(4-methoxy-2-nitrophenyl)-2-chloroacetamide (**2**) as a dark yellow solid (**2** has been reported previously [18]; for the X-ray structure of **1a**, see *Fig. 2*). Species **1a** and **2** were characterised by ESI-MS which showed ion peaks for the parent ion M^+ (**2**) or protonated parent ion $[M+H]^+$ (**1a**). In both cases, the ^{1}H-NMR revealed the three distinctive aromatic resonances together with two *s* for the acetamide CH_2 group and the MeO moiety. Since the spectra were obtained in $CDCl_3$ solutions, it was also possible to assign the amide resonance of **1a** and **2**, which showed dramatic differences (NH of **1a** at δ(H) *ca.* 9.2 and of **2** at δ(H) 11.5).

The 2-chloroacetamides **1a** and **2** were then coupled with tri(*tert*-butyl) 1,4,7,10-tetraazacyclododecane-1,4,7-triacetate [4] (which has previously been successfully

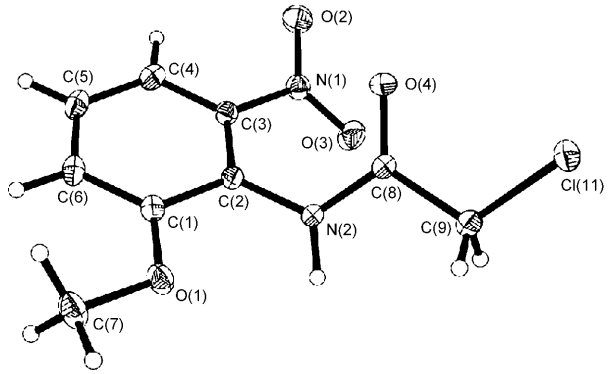

Fig. 2. *X-Ray-structure representation of* **1a**. Solvent molecules of crystallisation are omitted for clarity. Probability ellipsoids set at 50%.

employed to access a large range of functionalised DO3A-derived macrocyclic ligands; DO3A = 1,4,7,10-tetraazacyclododecane-1,4,7-triacetate), in the presence of one equiv. of KI and base, to give the intermediate triester derivatives, **E1** and **E2** (for formulas, see the corresponding **L1** and **L2**), in moderate yield. Purification was achieved by firstly removing unreacted triester by recrystallisation from toluene, and then by alumina-based column chromatography, the eluent CH_2Cl_2 removing unreacted chloroacetamide and CH_2Cl_2/MeOH 9:1 furnishing the product **E1** or **E2**. The triester intermediates were characterised by a range of spectroscopic techniques. The ESI-MS showed the expected peaks at m/z 723 for $[M+H]^+$. In the aromatic region of the ^{1}H-NMR spectra, there were minor shifts of the resonances when compared to the precursor 2-chloroacetamides: assignment of the amide H-atoms again revealed a far more deshielded NH environment for the *para*-isomer **E2** than for **E1**.

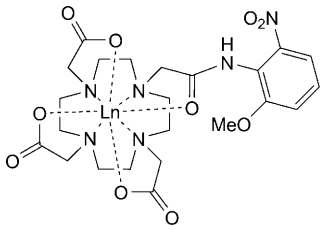

[Ln(**L1**)]

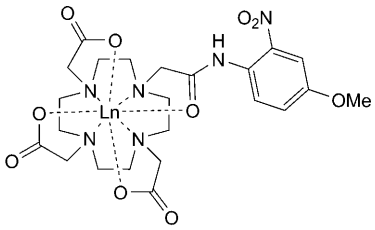

[Ln(**L2**)]

Single crystals suitable for X-ray diffraction were obtained for both functionalised triester intermediates **E1** and **E2** (*Figs. 3* and *4*). Although the data obtained for **E1** were of poorer quality (due to a weak data set, a large asymmetric unit, and a disordered *t*-Bu group), parameters associated with the provisional structure of **E1** are

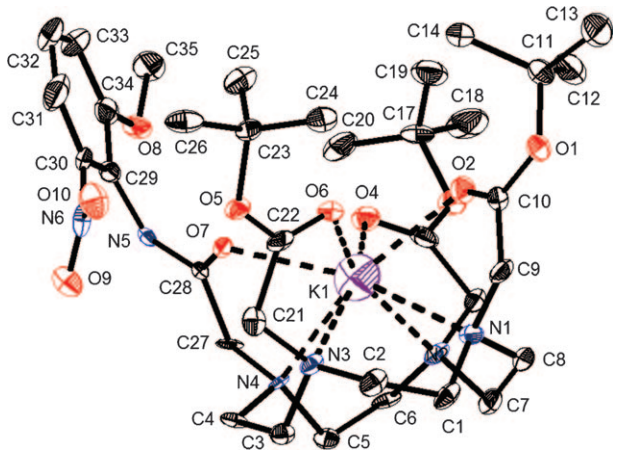

Fig. 3. *X-Ray-structure representation of* **E1**. Solvent molecules of crystallisation and counter ion are omitted for clarity. Probability ellipsoids set at 50%.

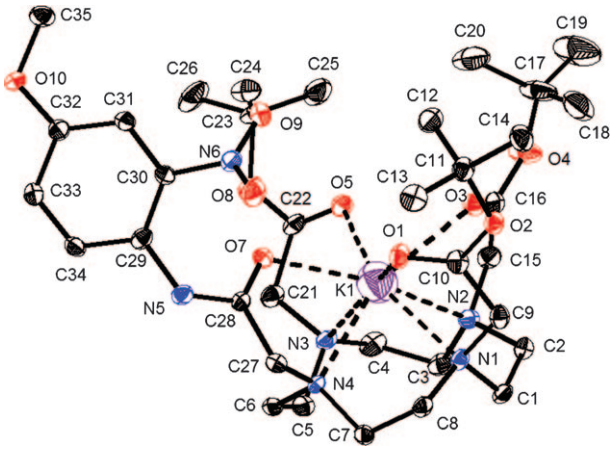

Fig. 4. *X-Ray-structure representation of* **E2**. Solvent molecules of crystallisation and counter ion are omitted for clarity. Probability ellipsoids set at 50%.

provided to allow confirmation and comparison of the basic structure. Crystals were grown from AcOEt/hexane solutions at $-20°$ or *via* vapor diffusion of Et_2O into concentrated $CHCl_3$ solutions. Parameters associated with the data collection of **E1** and **E2** are presented in *Table 1*. In both cases, the structural studies confirmed the proposed formulations with the protected ligands isolated as their potassium complexes, in accordance with previous reports on related triester [19] and triamide [6] derivatives. Both structures show the potassium ion coordinated by all four N-atoms of the macrocycle and by four C=O O-atom donors, one of which is from the *N*-arylacetamide moiety. For **E1**, the benzene ring is almost orthogonal to the amide group and as a result almost perpendicular to the N_4 plane of the macrocycle. The structure of **E2** revealed a twisted amide group which was not co-planar with the benzene ring and may be a consequence of potassium coordination of the amide.

The differences in coplanarity between the amide group and benzene ring would be expected to influence the degree of electronic conjugation throughout the system. It is likely that this structural variation between **E1** and **E2** accounts for the significant difference in the ^{1}H-NMR chemical shift of the amide H-atom: the δ(NH) of **E2** was shifted downfield by *ca.* 2 ppm suggesting a far more electron-deficient amide and, therefore, a more conjugated chromophore.

In both cases, the complex cation is charge-balanced by a single iodide counter anion (from KI). These X-ray structures are informative since we have previously shown analogous sodium complexes to be useful benchmarks for predicting the corresponding lanthanide coordination environment [19]. This is of particular use when interpreting the luminescence behavior of the lanthanide complexes where an understanding of the coordination sphere is of paramount importance. In these cases, it would suggest that a lanthanide complex of these ligands would favor the eight-coordinate binding mode where the amide C=O participates in the first coordination sphere.

Table 1. *Crystallographic Data of Compounds* **1a**, **1b**, **E1**, *and* **E2**[a])

	1a	**1b**	**E1**	**E2**
Empirical formula	$C_9H_9ClN_2O_4$	$C_8H_7ClN_2O_4$	$C_{35}H_{58}IKN_6O_{10} \cdot H_2O \cdot 0.75\ C_4H_8O_2$	$C_{35}H_{58}IKN_6O_{10} \cdot 0.75\ H_2O$
M_r	244.63	230.61	971.96	902.39
Crystal dimensions [mm]	$0.27 \times 0.22 \times 0.15$	$0.20 \times 0.09 \times 0.09$	$0.3 \times 0.22 \times 0.06$ mm^3	$0.22 \times 0.16 \times 0.06$
Temperature [K]	100(2)	100(2)	150(2)	150(2)
Wavelength [Å]	0.71073	0.71073	0.71073	0.71073
Crystal system	monoclinic	monoclinic	triclinic	monoclinic
Space group	*P*2(1)/*c*	*P*2(1)/*n*	*P*-1	*C*2/*c*
Z	4	4	4	8
Unit cell dimensions				
a [Å]	4.6925(3)	6.2783(6)	16.9830(7)	21.3350(4)
b [Å]	14.8214(8)	14.9977(13)	17.0630(8)	23.2170(5)
c [Å]	14.9223(10)	9.8799(9)	21.3680(9)	17.8310(4)
α [°]	90	90	101.560	90.00
β [°]	97.287(4)	100.430(4)	105.440(7)	97.0750(10)
γ [°]	90	90	111.950	90.00
Volume [Å^3]	1029.45(11)	914.92(14)	5215.1(4)	8765.1(3)
D_x [g cm^{-3}]	1.578	1.674	1.238	1.368
Absorption coefficient	4.289	4.289	4.439	4.439
F(000)	504	472	3756	3756
θ Range for data collection [°]	2.75 – 27.4	2.50 – 27.65	1.05 – 21.97	2.8 – 27.54
Reflections collected	3627	2128	12477	8918
Independent reflections	3083	1962	8564	5365
Goodness-of-fit on *F*	1.059	1.070	1.413	1.027
Final *R* indices ($I > 2\sigma(I)$) (R_1; wR_2)	0.0377; 0.1050	0.0285; 0.0782	0.1265; 0.1768	0.0755; 0.1852
R indices (all data) (R_1; wR_2)	0.0446; 0.1093	0.0311; 0.0803	0.3493; 0.3853	0.1363; 0.2174

[a]) The structure was refined on F_o^2 with all data.

Finally, the *tert*-butyl ester → carboxylic acid deprotection step (CF_3COOH, CH_2Cl_2) [4] occurred without cleavage of the chromophore from the macrocyclic framework, yielding the free triacid ligands **L1** and **L2**. These hygroscopic species were characterised by MS which showed clusters of peaks corresponding to ($[M + K]^+$) and the isotopomers of ($[M + Cu]^+$) in each case, (presumably as a consequence of scavenging trace Cu contamination within our mass spectrometry set-up). The ^{1}H-NMR spectra again showed resonances attributable to the presence of the macrocyle and appended chromophore and diagnostically established the absence of the *t*-Bu resonances at δ(H) *ca.* 1.3 – 1.4. The $^{13}C\{^1H\}$-NMR spectra also revealed the appropriate resonances associated with the ligands together with the presence of CF_3COOH, confirmed *via* characteristic *q*s observed at δ(C) *ca.* 118 and 163. Previous reports [19][20] have noted the formation of CF_3COOH adducts following the deprotection procedure described above. Accordingly, the CF_3COOH adducts were quantitatively established by elemental analyses which showed *ca.* two molecules of CF_3COOH per molecule of ligand, again in agreement with previous observations.

The lanthanide complex [Ln(**L1**)] was isolated as pale cream powder and [Ln(**L2**)] as olive yellow powder; both were typically sensitive to moisture. High-resolution accurate MS were obtained for each complex, confirming the isolation of the desired species, and in each case showing the characteristic isotopic distribution representative of the lanthanide.

An assessment of the absorption properties of the two chromophores revealed that **2** possessed a red-shifted absorption (λ_{max} 373 nm, ε 2100 mol^{-1} dm^3 cm^{-1}) when compared to **1a** (λ_{max} 323 nm, ε 2200 mol^{-1} dm^3 cm^{-1}). In each case, this long-wavelength transition was assigned to an intraligand component, based upon a $^1\pi\pi^*$ state. The reasons for the differing absorption behavior should be related to the overall conjugation of the substituted aryl unit. The conjugation of the amide group may be assessed, therefore, by considering a combination of structural and spectroscopic handles. For the *para*-MeO derivatives [Ln(**L2**)], the more closely planar *N*-arylacetamide unit appears to extend the conjugation of the chromophore, resulting in a red-shifted absorption and an electron-deficient environment at the amide group (as determined from ^{1}H-NMR).

Density-Functional-Theory Calculations. Since the differing spectroscopic characteristics of the chromophores arise from the *ortho- vs. para*-substitution, we undertook a complementary density-functional-theory (DFT) study to probe the energetic consequences of aryl substitution in these systems. Initially, the structure of the 2-chloroacetamide $\mathbf{1b}_{qm}$ was computed and the metric parameters compared to those obtained from the crystallographic study of **1b** (*Fig. 1*). The bond lengths and angles (*Table 2*) are generally in very good agreement with the measured X-ray data; this comparison lends support to the reliability of the calculation methods applied in this study. Interestingly, where the calculated model differs significantly from the X-ray data is when considering the torsion angles associated with the amide and nitro substituents. Both models minimise the steric clash between the amide and nitro groups by twisting them out of the plane defined by the benzene ring. In contrast to the calculations, the measured X-ray structural data shows that the molecule twists the amide group significantly more ($>60°$) than predicted, thereby allowing the nitro group to reside closer to coplanarity with the benzene ring.

Table 2. *Comparison of Calculated and Measured Parameters for the Structure of* **1b**

	Measured bond length [Å]	Calculated bond length [Å]
N(1)–C(6)	1.4711(17)	1.469
N(1)–O(2)	1.2215(15)	1.223
N(1)–O(3)	1.2344(15)	1.223
O(1)–C(2)	1.3491(15)	1.360
N(2)–C(1)	1.4177(15)	1.397
Cl(1)–C(8)	1.7787(13)	1.799
O(4)–C(7)	1.2323(16)	1.217
N(2)–C(7)	1.3340(16)	1.366
	Measured bond angle [°]	Calculated bond angle [°]
O(2)–N(1)–O(3)	122.99(11)	125.24
C(1)–N(2)–C(7)	122.85(11)	124.33
C(7)–C(8)–Cl(1)	114.84(9)	116.74
	Measured torsion angle [°]	Calculated torsion angle [°]
O(4)–C(7)–C(8)–Cl(1)	170.9(1)	166.75
C(6)–C(1)–N(2)–C(7)	60.49(17)	44.26
O(2)–N(1)–C(6)–C(1)	19.98(17)	33.51

The model systems *N*-(2-methoxy-6-nitrophenyl)acetamide (**3**$_{qm}$) and *N*-(4-methoxy-2-nitrophenyl)acetamide (**4**$_{qm}$) were studied by using DFT (B3PW91) methods; the computed structures of **4**$_{qm}$ and **3**$_{qm}$ are displayed in *Fig. 5*. In **4**$_{qm}$, the amide and nitro groups lie *ca.* coplanar to the benzene ring as would be expected for a fully delocalised system. This observation is further supported by the fact that rotation of the amide moiety has an activation barrier of *ca.* 10 kcal mol^{-1}, consistent with the disruption of a π-delocalised system. This is comparable with the calculated activation barrier to rotation of *ca.* 5 kcal mol^{-1} reported by *Kawauchi* and co-workers [21] for a system containing an aromatic ring on both sides of the amide linkage; the possibility of delocalising the C=O over a benzene ring, in addition to the N-based lone pair, is likely to be the reason for the reduced activation barrier compared to the system described herein. The ground-state structure of **3**$_{qm}$ possessed a nonplanar arrangement of both the amide and nitro groups (as observed in the calculated and measured structures of **1b**), with the amide showing significantly more deviation from planarity compared to the nitro group; although these groups are not perpendicular, the deviation from

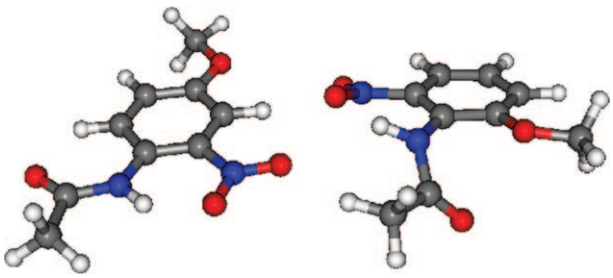

Fig. 5. *Calculated structures of* **4**$_{qm}$ (left) *and* **3**$_{qm}$ (right)

planarity is nevertheless expected to reduce the extent of the delocalisation. The likely cause of the nonplanarity of the amide group is most probably due to the steric repulsion imposed by the two *ortho*-substituents. The activation barrier associated with rendering the amide planar with the ring is 11 kcal mol^{-1}.

The energy gap between the HOMO and LUMO of $\mathbf{3}_{qm}$ and $\mathbf{4}_{qm}$ is affected by the extent of π-delocalisation over the system, since the HOMO and LUMO are associated with the aromatic ring and π-bonding to both the amide and nitro groups (*Fig. 6*). This energy difference was, therefore, estimated by considering the relative energies of the HOMO and LUMO in both $\mathbf{3}_{qm}$ and $\mathbf{4}_{qm}$. In $\mathbf{4}_{qm}$, the HOMO – LUMO gap is 3.46 eV (359 nm), whereas in $\mathbf{3}_{qm}$ (where the π-delocalisation has been disrupted) the value increases to 3.73 eV (333 nm). Obviously, this model system lacks the structural complexity of the free ligands **L1** and **L2** or the complexes, but the difference ($\Delta E \approx$ 2200 cm^{-1}) is in reasonable agreement, in both direction and magnitude, with that experimentally observed (from UV/VIS studies) for the macrocyclic triesters **E1** and **E2** (2870 cm^{-1}). It is likely, therefore, that the absorption properties of the *ortho*- and *para*-substituted chromophoric species are dependent upon the extent of π-delocalisation. This is a direct consequence of the steric accommodation of the amide substituent, resulting in the electronically preferred planar arrangement of the amide group being far more likely in the *para* isomer. Additionally, it is important to note that the amide substitutent is likely to become even more electron-withdrawing when coordinated to the strongly *Lewis* acidic lanthanide ions, although the act of coordination will also effect the torsion angle of the *N*-arylacetamide.

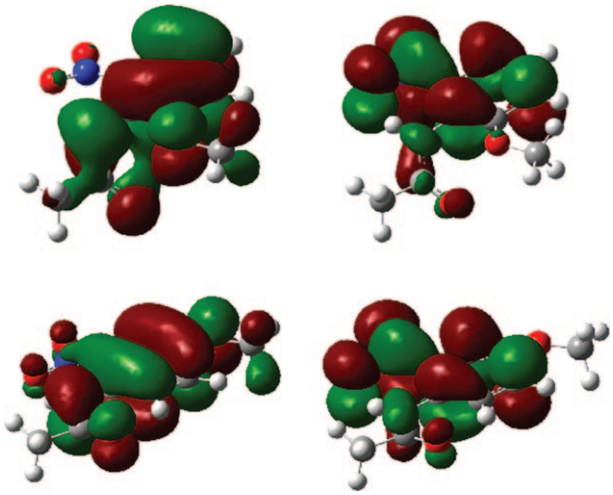

Fig. 6. *HOMO* (left) *and LUMO* (right) *of* $\mathbf{3}_{qm}$ (top) *and* $\mathbf{4}_{qm}$ (bottom)

Luminescence Properties of the Complexes. The potentially emissive $^6P_{7/2}$ state of Gd^{III} is at high UV energies (*ca.* 32000 cm^{-1}) [22]. The Gd^{III} complexes were found to be nonemissive at room temperature, but in EtOH at 77 K, they were luminescent. Following excitation at 290 nm, the time-gated phosphorescence spectra of both complexes [Gd(**L1**)] and [Gd(**L2**)] showed a broad, structureless emission with a

maximum intensity at *ca.* 440 nm. In each case, the high-energy onset of the peak allowed estimation of the triplet energy of the chromophore; *ca.* 23400 cm^{-1} in both cases and thus at sufficient energy to sensitise the lanthanide ions used in this study. The Nd^{III}, Eu^{III}, and Yb^{III} complexes each gave emission spectra characteristic of the coordinated ion and consistent with its inclusion in the macrocyclic binding site. Time-resolved measurements were obtained with H_2O/D_2O solutions of the complexes (*Table 3*). The excitation wavelengths for each system were indirect irradiation (λ_{ex} 355 nm) for Nd^{III} and Yb^{III} and both direct and indirect irradiation for Eu^{III} (λ_{ex} 396 and 320 nm). For each case, the decay profile was analysed as a single exponential component, indicative of a single emissive species. The measured lifetimes can be utilised to deduce the inner-sphere coordination environment, in terms of the degree of lanthanide hydration, q ($q = A[(k_{H2O} - k_{D2O}) - B]$: for Eu^{III}, $A = 1.25$ ms and $B = 0.25$ ms^{-1}; for Yb^{III}, $A = 1$ µs and $B = 0.2$ $µs^{-1}$; for aqueous Nd^{III}, $q = 130$ ($k_{H2O} - k_{D2O}) - 0.4$) [23] presented in *Table 3*. From these values, we conclude that the amide C=O is coordinated to the lanthanide in each case as expected for eight-coordinate ligands [22][23] of this type where q is *ca.* ≤ 1. It is noteworthy that despite parameters derived from related aminocarboxylate studies [23], both Nd^{III} species possess a slightly lower than expected q value. In fact, the values obtained in this study are more akin to those reported for the *Lehn*-cryptand complex of Nd^{III} (*cf.* $\tau_{H2O} = 100$ ns, $q = 0.46$) [24] where proximate C–H quenching modes are limited. Near-IR steady-state spectra were obtained with excitation wavelengths between 320 and 370 nm. The Nd^{III} complex displayed near-IR emission dominated by a peak at 1058 nm ($^4F_{3/2} \rightarrow {}^4I_{11/2}$) (utilising a longpass filter prevented the observation of the higher-energy $^4F_{3/2} \rightarrow {}^4I_{9/2}$ transition) with a weaker feature at *ca.* 1340 nm, corresponding to decay of the $^4I_{13/2}$ transition. The steady-state emission spectra of [Yb(**L1**)] and [Yb(**L2**)] (*Fig. 7*) gave spectral profiles typical of Yb^{III} with a peak at 975 nm ($^2F_{5/2} \rightarrow {}^4F_{7/2}$) together with a broadened, vibronic component to low energy, below 10000 cm^{-1}.

Table 3. *Luminescence Lifetimes of the Lanthanide Complexes*[a])[b])

	τ_H [µs]	τ_D [µs]	q[c])
[Nd(**L1**)]	0.095	0.327	0.6
[Eu(**L1**)]	429	922	1.2
[Yb(**L1**)]	0.776	7.629	1.0
[Nd(**L2**)]	0.085	0.270	0.6
[Eu(**L2**)]	530	1507	1.2
[Yb(**L2**)]	0.802	8.611	0.9

[a]) Measurements obtained in H_2O and D_2O with λ_{ex} 320 or 355 nm. [b]) Lifetimes are associated with a ±10% error. [c]) Estimated inner-sphere hydration number.

Conclusions. – This article discusses the use of *N*-(nitrophenyl)acetamide-derived chromophores as sensitisers in emissive lanthanide complexes. In comparison to simple phenol-derived species, the chromophores presented here display moderately red-shifted absorption bands between 300 and 350 nm allowing each chromophore to sensitise a range of lanthanide ions in aqueous solution. Through experimental

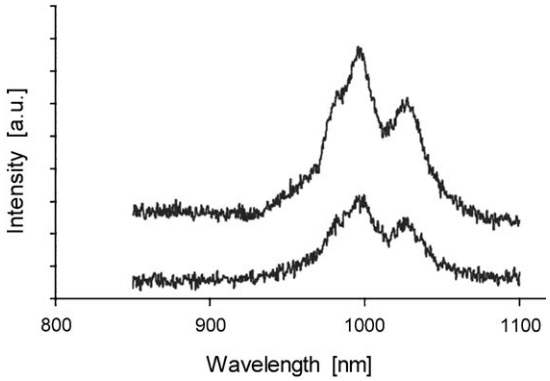

Fig. 7. *Steady-state emission spectra of* [Yb(**L1**)] (top) *and* [Yb(**L2**)] (bottom) *in* D_2O (λ_{ex} 330 nm)

spectroscopic studies and complimentary DFT calculations, attempts to rationalise the differences in absorption properties between the two isomeric forms of the chromophores were made. This investigation shows that the steric demands of the nitro and aminocarbonyl substituent at the benzene ring cause varying disruptions in the π-delocalisation throughout the chromophore and thus, the position of these substituents at the benzene moiety dictates the HOMO – LUMO energy gap. In this context, the extended conjugation of the *para*-MeO chromophore possesses a more red-shifted IL $^1\pi-\pi^*$ transition allowing longer-wavelength sensitization.

The *EPSRC* are thanked for support (EP/E048390/1) together with the Universities of Cardiff and Sheffield. The *EPSRC* MS National Service at Swansea is also gratefully acknowledged.

Experimental Part

1. *General.* UV/VIS Spectra: *Jasco 570* spectrophotometer; λ_{max} (ε / mol^{-1} dm^3 cm^{-1}) in nm. IR Spectra: *Varian 7000* FT-IR spectrometer; $\tilde{\nu}_{max}$ in cm^{-1}. NMR Spectra: *Bruker DPX* at 400 MHz; δ in ppm, *J* in Hz. ESI-MS: *Waters LCT Premier XE* in MeOH; in *m*/*z* (rel. %).

2. *Precursors, Ligands, and Corresponding Lanthanide Complexes.* 2.1. *2-Chloroacetamides: General Procedure.* A large excess (*ca.* 3 equiv.) of 2-chloroacetyl chloride was added under stirring to a soln. of the substituted aniline in MeCN, and the mixture was stirred for 1 h. The solvent was evaporated, and AcOEt was added. The org. phase was washed with H_2O, dried ($MgSO_4$), and concentrated: title compounds in high yield (typically 95%). The 2-chloroacetamides were used without further purification.

2-Chloro-N-*(2-methoxy-6-nitrophenyl)acetamide* (**1a**): Pale yellow crystals. Yield 97%. UV/VIS: 323 (2173). IR ($CHCl_3$): 1698 (C=O), 1512 (NO_2). ^{1}H-NMR ($CDCl_3$): 3.90 (*s*, MeO); 4.13 (*s*, CH_2Cl); 7.12 (*d*, 1 arom. H); 7.28 (*t*, 1 arom. H); 7.48 (*d*, 1 arom. H); 9.2 (br. *s*, NH). ESI-MS (pos.): 245 ($[M+H]^+$).

2-Chloro-N-*(4-methoxy-2-nitrophenyl)acetamide* (**2**): Dark yellow crystals. Yield 93%. UV/VIS: 373 (2091). IR ($CHCl_3$): 1694 (C=O), 1514 (NO_2). ^{1}H-NMR ($CDCl_3$): 3.81 (*s*, MeO); 4.16 (*s*, CH_2Cl); 7.18 (*s*, 1 arom. H); 7.64 (*s*, 1 arom. H); 8.58 (*d*, 1 arom. H); 11.5 (br. *s*, NH). ESI-MS (pos.): 244 (M^+).

2.2. *Protected Ligand Precursors: General Procedure.* The 2-chloroacetamide **1a** (1.5 equiv.) was added to a mixture of the bromide salt of tris(1,1-dimethylethyl) 1,4,7,10-tetraazacyclododecane-1,4,7-triacetate (1 equiv.), Et_3N (3 equiv.), and KI (1 equiv.) in MeCN, and the mixture was heated to reflux for 48 h. The soln. was filtered and concentrated, and the crude residue was purified by column chromatography (alumina, CH_2Cl_2, then CH_2Cl_2/MeOH 9:1).

Tris(1,1-dimethylethyl) 10-{2-[(2-Methoxy-6-nitrophenyl)amino]-2-oxoethyl}-1,4,7,10-tetraazacyclododecane-1,4,7-triacetate (**E1**): Brown oil. Yield 51%. UV/VIS: 220 (10799), 328 (709). IR ($CHCl_3$):

1727 (C=O), 1682 (NC=O), 1522 (N=O). ^{1}H-NMR ($CDCl_3$): 1.33 (*s*, 3 $COOCMe_3$); 1.90–3.74 (br. *m*, 24 H, CH_2 ring, NCH_2COO, NCH_2CON); 3.84 (*s*, MeO); 7.08 (*d*, 1 arom. H); 7.19 (*m*, 1 arom. H); 7.36 (*d*, 1 arom. H); 9.21 (br. *s*, NH). ESI-MS (pos.): 723 ($[M + H]^+$).

Tris(1,1-dimethylethyl) 10-{2-[(4-Methoxy-2-nitrophenyl)amino]-2-oxoethyl}-1,4,7,10-tetraazacyclododecane-1,4,7-triacetate (**E2**): Brown oil. Yield 67%. UV/VIS: 239 (87185), 362 (14267). IR ($CHCl_3$): 1732 (C=O), 1518 (N=O). NMR ($CDCl_3$): 1.35 (*s*, 3 $COOCMe_3$); 1.88–3.68 (br. *m*, 24 H, CH_2 ring, NCH_2COO, NCH_2CON); 3.76 (*s*, MeO); 7.01 (*d*, 1 arom. H); 7.36 (*s*, 1 arom. H); 7.81 (*d*, 1 arom. H); 11.1 (br. *s*, NH). ESI-MS (pos.): 723 ($[M + H]^+$).

2.3. *Deprotection of Ligands: General Procedure.* The protected ligand precursor was added to CF_3COOH/CH_2Cl_2 1:1, and the mixture was stirred at r.t. overnight. The solvent was evaporated, and the residue was redissolved three times in MeOH to eliminate excess acid. The residue was then dissolved in the minimum volume of MeOH and added dropwise under stirring to Et_2O at 0°. The precipitate was filtered and dried to give the deprotected ligand.

10-{2-[(2-Methoxy-6-nitrophenyl)amino]-2-oxoethyl}-1,4,7,10-tetraazacyclododecane-1,4,7-triacetic Acid (**L1**): Yellow powder. ^{1}H-NMR (D_2O): 2.95–4.05 (br. *m*, 27 H, CH_2 ring, NCH_2COO, NCH_2CON, MeO); 7.32–7.50 (overlapping, 3 arom. H). ^{13}C-NMR (101 MHz, D_2O): 49.3 (br.); 55.1 (br.); 57.0 (MeO); 57.8; 115.2; 117.0; 117.8 (*q*, *C*F_3COOH); 128.6; 145.6; 152.1; 154.5; 163.2 (*q*, CF_3*C*OOH); 174.5 (br., CO). ESI-MS (pos.): 593 ($[M+K]^+$). Anal. calc. for $C_{23}H_{34}N_6O_{10}\cdot(CF_3COOH)_2$ (782.60): C 41.44, H 4.64, N 10.74; found C 41.21, H 5.11, N 10.22.

10-{2-[(4-Methoxy-2-nitrophenyl)amino]-2-oxoethyl}-1,4,7,10-tetraazacyclododecane-1,4,7-triacetic Acid (**L2**): Yellow powder. ^{1}H-NMR (D_2O): 2.7–4.1 (br. *m*, 27 H); 3.81 (*s*, MeO); 7.30–7.49 (overlapping *m*, 3 arom. H); 7.51 (*d*, $^1J = 8.0$, 1 arom. H). ^{13}C-NMR (101 MHz, D_2O): 49.4 (br.); 53.4 (br.); 57.0; 57.8; 62.0; 115.2; 117.8 (*q*, *C*F_3COOH); 128.5; 145.6; 154.5; 163.2 (*q*, CF_3*C*OOH); 165.2; 174.7; 175.0 (CO). ESI-MS (pos.): 593 ($[M+K]^+$), 617 ($[M+Cu]^+$). Anal. calc. for $C_{23}H_{34}N_6O_{10}\cdot(CF_3COOH)_2$ (782.60): C 41.44, H 4.64, N 10.74; found C 41.15, H 5.40, N 10.28.

2.4. *Lanthanide Complexes: General Procedure.* A mixture of the ligand and either $Ln(OTf)_3$ or $Yb(NO_3)_3$ was stirred in MeOH at 50° for 24 h. The soln. was concentrated and then added dropwise under stirring to Et_2O at 0°. The precipitate was filtered, washed with Et_2O, and dried to give the lanthanide complex.

{10-{2-[(2-Methoxy-6-nitrophenyl)amino]-2-(oxo-κO)ethyl}-1,4,7,10-tetraazacyclododecane-1,4,7-triacetato(3-)-κN^1,κN^4,κN^7,κN^{10},κO^1,κO^4,κO^7}neodymium ([Nd(**L1**)]): Pale yellow powder. UV/VIS: 209 (8551), 327 (964). IR (nujol): 1600, 1645 (C=O). ESI-MS (pos.): 694 ($[M+H]^+$). HR-ESI-MS (pos.): 694.1259 ($[M+H]^+$, $C_{23}H_{32}N_6{}^{142}NdO_{10}^+$; calc. 694.1252).

{10-{2-[(2-Methoxy-6-nitrophenyl)amino]-2-(oxo-κO)ethyl}-1,4,7,10-tetraazacyclododecane-1,4,7-triacetato(3-)-κN^1,κN^4,κN^7,κN^{10},κO^1,κO^4,κO^7}europium ([Eu(**L1**)]): Pale yellow powder. UV/VIS: 210 (8870), 325 (1014). IR (nujol): 1599, 1648 (C=O). ESI-MS (pos.): 703 ($[M+H]^+$). HR-ESI-MS (pos.): 703.1383 ($[M+H]^+$, $C_{23}H_{32}{}^{151}EuN_6O_{10}^+$; calc. 703.1373).

{10-{2-[(2-Methoxy-6-nitrophenyl)amino]-2-(oxo-κO)ethyl}-1,4,7,10-tetraazacyclododecane-1,4,7-triacetato(3-)-κN^1,κN^4,κN^7,κN^{10},κO^1,κO^4,κO^7}gadolinium ([Gd(**L1**)]): Pale yellow powder. UV/VIS: 210 (9381), 324 (1143). IR (nujol): 1601, 1635 (C=O). ESI-MS (pos.): 707 ($[M+H]^+$). HR-ESI-MS (pos.): 707.1397 ($[M+H]^+$, $C_{23}H_{32}{}^{151}GdN_6O_{10}^+$; calc. 707.1401).

{10-{2-[(2-Methoxy-6-nitrophenyl)amino]-2-(oxo-κO)ethyl}-1,4,7,10-tetraazacyclododecane-1,4,7-triacetato(3-)-κN^1,κN^4,κN^7,κN^{10},κO^1,κO^4,κO^7}ytterbium ([Yb(**L1**)]): Pale yellow powder. UV/VIS: 214 (15378), 321 (1022). IR (nujol): 1598, 1630 (C=O). ESI-MS (pos.): 722 ($[M+H]^+$). HR-ESI-MS (pos.): 722.1520 ($[M+H]^+$, $C_{23}H_{32}N_6O_{10}{}^{170}Yb^+$; calc. 722.1522).

{10-{2-[(4-Methoxy-2-nitrophenyl)amino]-2-(oxo-κO)ethyl}-1,4,7,10-tetraazacyclododecane-1,4,7-triacetato(3-)-κN^1,κN^4,κN^7,κN^{10},κO^1,κO^4,κO^7}neodymium ([Nd(**L2**)]): Yellow powder. UV/VIS: 232 (11321), 340 (1000). IR (nujol): 1607, 1635 (C=O). ESI-MS (pos.): 694 ($[M+H]^+$). HR-ESI-MS (pos.): 694.1249 ($[M+H]^+$, $C_{23}H_{32}N_6{}^{142}NdO_{10}^+$; calc. 694.1252).

{10-{2-[(4-Methoxy-2-nitrophenyl)amino]-2-(oxo-κO)ethyl}-1,4,7,10-tetraazacyclododecane-1,4,7-triacetato(3-)-κN^1,κN^4,κN^7,κN^{10},κO^1,κO^4,κO^7}europium ([Eu(**L2**)]): Yellow powder. UV/VIS: 233 (9212), 338 (1139). IR (nujol): 1603, 1638 (C=O). ESI-MS (pos.): 703 ($[M+H]^+$). HR-ESI-MS (pos.): 703.1375 ($[M+H]^+$, $C_{23}H_{32}{}^{153}EuN_6O_{10}^+$; calc. 703.1373).

{10-{2-[(4-Methoxy-2-nitrophenyl)amino]-2-(oxo-κO)ethyl}-1,4,7,10-tetraazacyclododecane-1,4,7-triacetato(3-)-κN^1,κN^4,κN^7,κN^{10},κO^1,κO^4,κO^7}gadolinium ([Gd(**L2**)]): Yellow powder. UV/VIS: 231 (11393), 338 (1182). IR (nujol): 1598, 1640 (C=O). ESI-MS (pos.): 706 ($[M+H]^+$). HR-ESI-MS (pos.): 706.1383 ($[M+H]^+$, $C_{23}H_{32}{}^{154}GdN_6O_{10}^+$; calc. 706.1383).

{10-{2-[(4-Methoxy-2-nitrophenyl)amino]-2-(oxo-κO)ethyl}-1,4,7,10-tetraazacyclododecane-1,4,7-triacetato(3-)-κN^1,κN^4,κN^7,κN^{10},κO^1,κO^4,κO^7}ytterbium ([Yb(**L2**)]): Yellow powder. UV/VIS: 214 (13870), 340 (1164). IR (nujol): 1635, 1674 (C=O). ESI-MS (pos.): 722 ($[M+H]^+$). HR-ESI-MS (pos.): 722.1521 ($[M+H]^+$, $C_{23}H_{32}N_6O_{10}{}^{170}Yb^+$; calc. 722.1522).

Structure Analysis and Refinement[1]). The structure was solved by direct methods with SHELXS-97 and was completed by iterative cycles of ΔF syntheses and full-matrix least-squares refinement. All non-H-atoms were refined anisotropically, and difference *Fourier* syntheses were employed in positioning idealised H-atoms and were allowed to ride on their parent C-atoms. All refinements were against F^2 and used SHELX-97 [25].

DFT. All calculations were performed on the Gaussian 03 suite of programs [26]. Calculations were carried out with the hybrid B3PW91 functional, with the 6–31G(d,p) basis set for all atoms. Geometry optimisations were initially performed without geometry restraints, followed by frequency calculations to ascertain the nature of the resulting structure (minimum *vs.* transition state). Molecular images were created with the Molekel program [27].

REFERENCES

[1] J. C. G. Bünzli, C. Piguet, *Chem. Soc. Rev.* **2005**, *34*, 1048; T. Gunnlaugsson, J. P. Leonard, *Chem. Commun.* **2005**, 3114; S. Faulkner, S. J. A. Pope, B. P. Burton-Pye, *Appl. Spectrosc. Rev.* **2005**, *40*, 1.

[2] F. Kielar, G. L. Law, E. J. New, D. Parker, *Org. Biomol. Chem.* **2008**, *6*, 2256; B. S. Murray, E. J. New, R. Pal, D. Parker, *Org. Biomol. Chem.* **2008**, *6*, 2085; J. Yu, D. Parker, R. Pal, R. A. Poole, M. J. Cann, *J. Am. Chem. Soc.* **2006**, *128*, 2294; C. P. Montgomery, D. Parker, L. Lamarque, *Chem. Commun.* **2007**, 3841; S. Pandya, J. Yu, D. Parker, *Dalton Trans.* **2006**, 2757; A.-S. Chauvin, C. Vandevyer, S. Comby, J. C. G. Bünzli, *Chem. Commun.* **2007**, 1716; D. Parker, R. Pal, *Chem. Commun.* **2007**, 474; A. Beeby, S. W. Botchway, I. M. Clarkson, S. Faulkner, A. W. Parker, D. Parker, J. A. G. Williams, *J. Photochem. Photbiol. B* **2000**, *57*, 83.

[3] J. Yu, D. Parker, R. Pal, R. A. Poole, M. J. Cann, *J. Am. Chem. Soc.* **2006**, *128*, 2294; C. P. Montgomery, D. Parker, L. Lamarque, *Chem. Commun.* **2007**, 3841.

[4] A. Dadbhoy, S. Faulkner, P. G. Sammes, *J.Chem. Soc., Perkin Trans. 2* **2002**, 348.

[5] S. Faulkner, M-C. Carrié, S. J. A. Pope, J. Squire, A. Beeby, P. G. Sammes, *Dalton Trans.* **2004**, 1405; S. J. A. Pope, *Polyhedron* **2007**, *26*, 4818; M. Main, J. S. Snaith, M. M. Meloni, M. Jauregui, D. Sykes, S. Faulkner, A. M. Kenwright, *Chem. Commun.* **2008**, 5212.

[6] M. Andrews, L. P Harding, R. H. Laye, S. J. A. Pope, *Polyhedron* **2008**, *27*, 2365.

[7] R. Van Deun, P. Fias, P. Nockemann, K. Van Hecke, L. Van Meervelt, K. Binnemans, *Inorg. Chem.* **2006**, *45*, 10416; M. K. Nah, S. G. Rho, H. K. Kim, J. G. Kang, *J. Phys. Chem. A* **2007**, *111*, 11437; R. Shyni, S. Biju, M. L. P. Reddy, A. H. Cowley, M. Findlater, *Inorg. Chem.* **2007**, *46*, 11025; A. M. Reynolds, B. R. Sculimbrene, B. Imperiali, *Bioconj. Chem.* **2008**, *19*, 588; N. M. Shavaleev, R. Scopelliti, F. Gumy, J. C. G. Bünzli, *Inorg. Chem.* **2008**, *47*, 9055; M. Albrecht, O. Osetska, J. Klankermayer, R. Fröhlich, F. Gumy, J. C. G. Bünzli, *Chem. Commun.* **2007**, 1834; M. H. V. Werts, J. W. Verhoeven, J. W. Hofstraat, *J. Chem. Soc., Perkin Trans. 2* **2000**, 433; A. Bodi, K. E. Borbas, J. I. Bruce, *Dalton Trans.* **2007**, 4352.

[8] D. Imbert, M. Cantuel, J.-C. G. Bünzli, C. Berardinelli, C. Piguet, *J. Am. Chem. Soc.* **2003**, *125*, 15698; T. Lazarides, G. M. Davies, H. Adams, C. Sabatini, F. Barigelletti, A. Barbieri, S. J. A. Pope, S. Faulkner, M. D. Ward, *Photochem. Photobiol. Sci.* **2007**, *6*, 1152.

[9] S. I. Klink, H. Keizer, F. C. J. M. van Veggel, *Angew. Chem., Int. Ed.* **2000**, *39*, 4319; M. D. Ward, *Coord. Chem. Rev.* **2007**, *251*, 1663; J.-M. Herrera, S. J. A. Pope, A. J. H. M. Meijer, T. L. Easun, H.

---

[1]) CCDC-723201–723204 contain the supplementary crystallographic data for **1a**, **1b**, **E1**, and **E2**. These data can be obtained free of charge *via* http://www.ccdc.cam.ac.uk/data_request/cif.

Adams, W. Z. Alsindi, X-Z. Sun, M. W. George, S. Faulkner, M. D. Ward, *J. Am. Chem. Soc.* **2007**, *128*, 11491; K. Senechal-David, S. J. A. Pope, S. Quinn, S. Faulkner, T. Gunnlaugsson, *Inorg. Chem.* **2006**, *45*, 10040.

[10] S. J. A. Pope, B. J. Coe, S. Faulkner, R. H. Laye, *Dalton Trans.* **2005**, 1482; S. J. A. Pope, B. J. Coe, S. Faulkner, *Chem. Commun.* **2004**, 1550.

[11] S. J. A. Pope, B. J. Coe, S. Faulkner, E. V. Bichenkova, X. Yu, K. T. Douglas, *J. Am. Chem. Soc.* **2004**, *126*, 9490; T. Riis-Johannessen, N. Dupont, G. Canard, G. Bernardinelli, A. Hauser, C. Piguet, *Dalton Trans.* **2008**, 3661; S. G. Baca, S. J. A. Pope, H. Adams, M. D. Ward, *Inorg. Chem.* **2008**, *47*, 3736; T. Lazarides, H. Adams, D. Sykes, S. Faulkner, G. Calogero, M. D. Ward, *Dalton Trans.* **2008**, 691; T. Lazarides, D. Sykes, S. Faulkner, A. Barbieri, M. D. Ward, *Chem. – Eur. J.* **2008**, *14*, 9389.

[12] P. Coppo, M. Duati, V. N. Kozhevnikov, J. W. Hofstraat, L. DeCola, *Angew. Chem., Int. Ed.* **2005**, *44*, 1806; M. Mehlstaubl, G. S. Kottas, S. Colella, L. De Cola, *Dalton Trans.* **2008**, 2385; F. F. Cheng, Z. Q. Bian, Z. W. Liu, D. B. Nie, Z. Q. Chen, C. H. Huang, *Inorg. Chem.* **2008**, *47*, 2507; F. F. Chen, Z. Q. Bian, B. Lou, E. Ma, Z. W. Liu, D. B. Nie, Z. Q. Chen, J. Bian, Z. N. Chen, C. H. Huang, *Dalton Trans.* **2008**, 5577; F. F. Chen, Z. Q. Bian, Z. W. Liu, D. B. Nie, Z. Q. Chen, C. H. Huang, *Inorg. Chem.* **2008**, *47*, 2507.

[13] N. Shavaleev, L. P. Moorcraft, S. J. A. Pope, Z. R. Bell, S. Faulkner, M. D. Ward, *Chem. – Eur. J.* **2003**, *8*, 5283; T. K. Ronson, T. Lazarides, H. Adams, S. J. A. Pope, D. Sykes, S. Faulkner, S. J. Coles, M. B. Hursthouse, W. Clegg, R. W. Harrington, M. D. Ward, *Chem. – Eur. J.* **2006**, *12*, 9299; F. Kennedy, N. M. Shavaleev, T. Koullourou, Z. R. Bell, J. C. Jeffery, S. Faulkner, M. D. Ward, *Dalton Trans.* **2007**, 1492; X. L. Li, L. X. Shi, L. Y. Zhang, H. M. Wen, Z. N. Chen, *Inorg. Chem.* **2007**, *46*, 10892; J. Ni, L. Y. Zhang, Z. N. Chen, *J. Org. Met. Chem.* **2009**, *694*, 339.

[14] N. M. Shavaleev, R. Scopelliti, F. Gumy, J. C. G. Bünzli, *Eur. J. Inorg. Chem.* **2008**, 1523.

[15] M. Woods, G. E. Kiefer, S. Bott, A. Castillo-Muzquiz, C. Eshelbrenner, L. Michaudet, K. McMillan, S. D. K. Mudigunda, D. Ogrin, G. Tirsco, S. Zhang, P. Zhao, A. D. Sherry, *J. Am. Chem. Soc.* **2004**, *126*, 924.

[16] Y. X. Zheng, M. Motevalli, R. H. C. Tan, I. Abrahams, W. P. Gillin, P. B. Wyatt, *Polyhedron* **2008**, *27*, 1503.

[17] A. Beeby, L. M. Bushby, D. Matteo, J. A. G. Williams, *J. Chem. Soc.*, *Dalton Trans.* **2002**, 48.

[18] F. Reverdin, *Helv. Chim. Acta* **1923**, *6*, 87.

[19] S. J. A. Pope, R. H. Laye, *Dalton Trans.* **2006**, 3108.

[20] S. J. A. Pope, V. Boote, A. M. Kenwright, S. Faulkner, *Dalton Trans.* **2003**, 3780.

[21] J. Nishikawa, T. Imase, M. Koike, K. Fukuda, M. Tokita, J. Watanabe, S. Kawauchi, *J. Mol. Struct.* **2005**, *741*, 221.

[22] D. Parker, J. A. G. Williams, *J. Chem. Soc., Perkin Trans. 2* **1996**, 1581; D. Parker, P. K. Senanayake, J. A. G. Williams, *J. Chem. Soc., Perkin Trans. 2* **1998**, 2129.

[23] A. Beeby, I. M. Clarkson, R. Dickins, S. Faulkner, D. Parker, L. Royle, A. S. de Sousa, J. A. G. Williams, M. Woods, *J. Chem. Soc., Perkin Trans. 2* **1999**, 493.

[24] S. Faulkner, A. Beeby, M. C. Carrie, A. Dadabhoy, A. M. Kenwright, P. G. Sammes, *Inorg. Chem. Commun.* **2001**, *4*, 187.

[25] SHELXL-PC Package, Bruker Analytical X-ray Systems, Madison, WI, 1998.

[26] M. J. Frisch, G. W. Trucks, H. B. Schlegel, G. E. Scuseria, M. A. Robb, J. R. Cheeseman, V. G. Zakrzewski, J. A. Montgomery Jr., R. E. Stratmann, J. C. Burant, S. Dapprich, J. M. Millam, A. D. Daniels, K. N. Kudin, M. C. Strain, O. Farkas, J. Tomasi, V. Barone, M. Cossi, R. Cammi, B. Mennucci, C. Pomelli, C. Adamo, S. Clifford, J. Ochterski, G. A. Petersson, P. Y. Ayala, Q. Cui, K. Morokuma, D. K. Malick, A. D. Rabuck, K. Raghavachari, J. B. Foresman, J. Cioslowski, J. V. Ortiz, A. G. Baboul, B. B. Stefanov, G. Liu, A. Liashenko, Y. Piskorz, A. Nanayakkara, C. Gonzalez, M. Challacombe, P. M. W. Gill, B. Johnson, W. Chen, M. W. Wong, J. L. Andres, M. Head-Gordon, E. S. Replogle, J. A. Pople, Gaussian 03, Revision B.03, 2003).

[27] Swiss National Computing Centre, Molekel 5.3, 2006.

Received March 24, 2009